A Novel Method for Generating Continuously Surfable Waves—Comparison of Predictions With Experimental Results

Steven A. Schmied
Australian Maritime College,
Launceston Tasmania Australia,
6 Edinburgh Street,
Hampton Victoria,
3188 Australia
e-mail: sschmie@tpg.com.au

Jonathan R. Binns
e-mail: j.binns@amc.edu.au

Martin R. Renilson[1]
Professor
e-mail: martin.renilson@hct.ac.ae

Giles A. Thomas
Associate Professor
e-mail: giles@amc.edu.au

Gregor J. Macfarlane
e-mail: g.macfarlane@amc.edu.au

Australian Maritime College,
Locked Bag 1395,
University of Tasmania,
Launceston Tasmania,
7250 Australia

Rene Huijsmans
Professor
Delft University of Technology,
Room Number 7-1-127,
Mekelweg 2,
Delft 2628CD,
The Netherlands
e-mail: R.H.M.Huijsmans@TUDelft.NL

In this paper, a novel idea to produce continuous breaking waves is discussed, whereby a pressure source is rotated within an annular wave pool, with the inner ring of the annulus having a sloping bathymetry to induce wave breaking. In order to refine the technique, work is being conducted to better understand the mechanics of surfable waves generated by moving pressure sources in restricted water. The pool aims to be capable of creating waves suitable for surfers from beginner to expert level, with an added benefit being by providing a safe learning environment, the overall surfing ability of the participants should be improved. The method of approach reported in this paper is the first stage of an experimental investigation of a novel method for generating continuously surfable waves utilizing a moving pressure source. The aim was to measure and assess the waves generated by two parabolic pressure sources and a wedge-shaped wavedozer (Driscoll, A., and Renilson, M. R., 1980, The Wavedozer. A System of Generating Stationary Waves in a Circulating Water Channel, University of Glasgow, Naval Architecture and Ocean Engineering, Glasgow, UK) for their suitability for future development of continuous breaking surfable waves. The tests were conducted at the University of Tasmania (UTas) Australian Maritime College (AMC) 100 m long towing tank. The predictions and experimental results for the wave height (H) at different values of depth Froude number (Fr_h) are presented in this paper. Finally, the preferred pressure source is determined based on the wave making energy efficiency and the quality of the waves for surfing.
[DOI: 10.1115/1.4023798]

Keywords: ship waves, model testing, wave pool, surfable waves

Introduction

Many surfers do not have the luxury of living near surf breaks, and must travel long distances in order to surf. As coastal populations increase, and surfing becomes more popular, existing surf breaks become overcrowded. Surfers have responded by traveling to more distant and remote locations to chase uncrowded and better waves [1], although this increases the cost of surfing and does nothing to reduce crowding at their home breaks. Another solution has been to build artificial reefs in the ocean; however, these still rely on natural wave conditions. A third solution is to develop new breaks and generate waves in a controlled environment: the wave pool.

Wave pools are not a new concept. In 1934, the Wembley Swimming Pool in London was the first to thrill its visitors with small artificial waves. In 1966, the first indoor surfers rode waist-high waves in the Summerland wave pool in Tokyo, Japan [2]. Since then, more surf pools have been built around the world, receiving somewhat mixed reviews from surfers. The original linear wave pools, where the waves are generated at one end and travel to a beach at the other end, try to mimic naturally occurring waves with piston-driven paddles or similar mechanical devices. Such man-made waves are not very appealing to surfers as the rides are short, and the waves weak and poorly shaped.

Some manufacturers bend the pool around a curve to concentrate the swell or shape the pool floor to improve the wave height [3]. Another method used to simulate surfing waves is to shoot a thin sheet of water over a wave shaped surface. However, this method does not provide an authentic surfing experience (a moving wave breaking along a shoreline) and, like the linear pools, generally only allow one rider at a time [4]. A third concept aims to draw an object through shallow water along a linear track, creating waves on each side [5]. Key deficiencies with these approaches involve both the lack of an authentic, scalable surfing wave motion of a moving wave breaking on a shoreline, and a limitation on the number of riders able to surf at one time (thus limiting the financial viability of the pool).

In order to find the solution to the problems defined above, a novel idea to produce continuous breaking waves has been patented [6,7], by Liquid Time Pty Ltd., whereby one or more pressure sources are rotated within an annular wave pool (see Figs. 1 and 2). A pressure source may be any object that disrupts the water surface, such as a ship hull or submerged body (submarine).

The inner ring of the annulus has a sloping bathymetry (e.g. a beach) to induce breaking of the waves (shown as originating at the pressure sources), with the break point following the circular path around the central island (shown as the dashed line) at a given water depth proportional to the wave height. The pool aims to be capable of creating waves suitable for surfers from beginner to expert level, with an added benefit being that by providing a safe learning environment, the overall surfing ability of the

[1]Currently employed as Dean, Maritime at the Higher Colleges of Technology, United Arab Emirates (UAE).

Contributed by the Ocean, Offshore, and Arctic Engineering Division of ASME for publication in the Journal of Offshore Mechanics and Arctic Engineering. Manuscript received September 23, 2011; final manuscript received August 13, 2012; published online May 22, 2013. Assoc. Editor: Daniel T. Valentine.

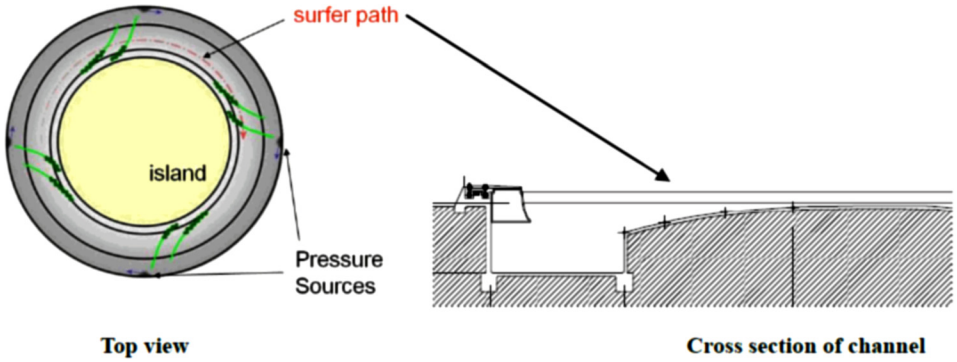

Fig. 1 Concept design for the efficient method of generating continuously surfable breaking waves using moving pressure sources

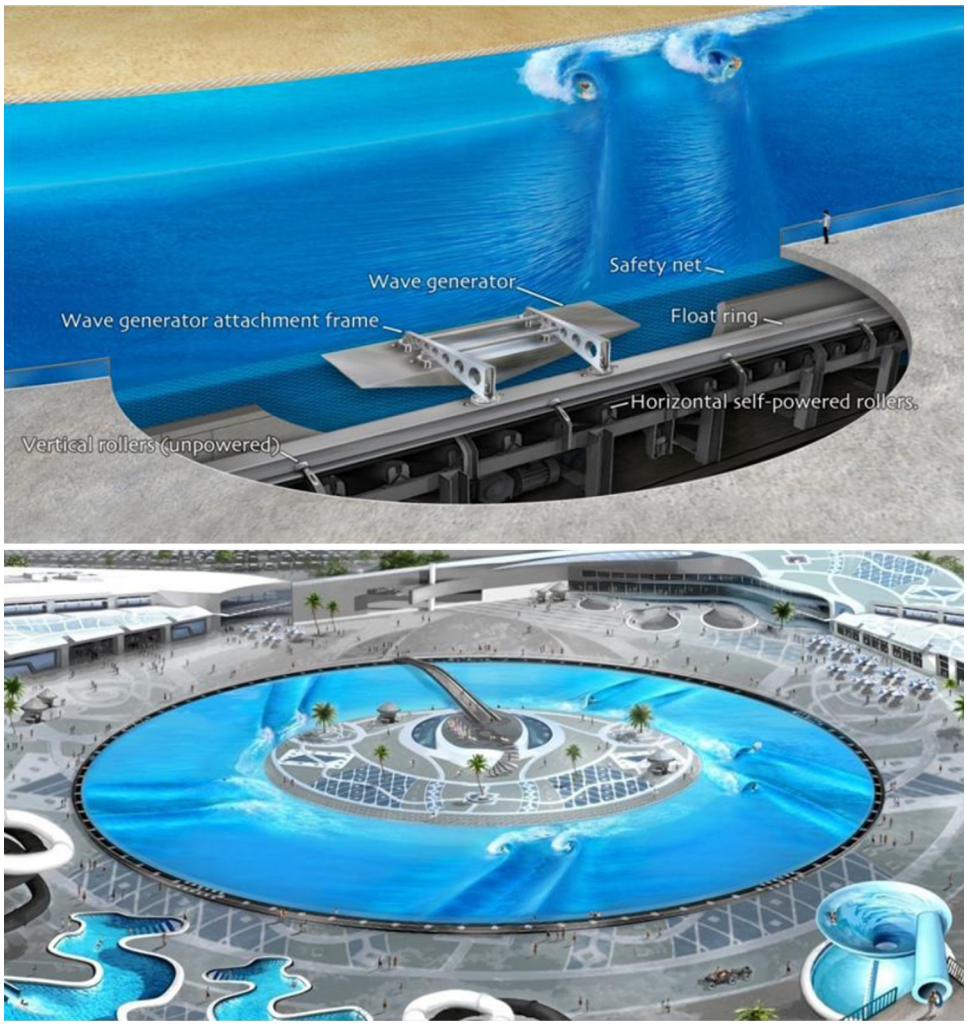

Fig. 2 Wave pool concept

participants should be improved. The concept was proven, at least for a linear track, using a fishing vessel generating waves in a river estuary, where the vessel traveled in a straight line close to the bank [8].

The quality of the waves generated by the pressure sources is critical for surfing. For the waves to be surfable, the waves should be smooth sinusoidal (not breaking) in shape. Only when the wave is triggered to break due to the presence of shallowing (sloping) bathymetry (e.g. a beach), will the surfer rides at or near the break point but out on the unbroken part of the wave. Thus, without the presence of a beach, the waves generated by the pressure source should remain unbroken. Commercially, it is also preferable to generate two or more approximately evenly sized waves to maximize the number of surfers that can ride per pressure source.

This paper reports on the first stage of an experimental investigation of a novel method for generating continuously surfable waves utilizing a moving pressure source. The aim was to measure and assess the waves generated by three different pressure sources for their suitability for future development of continuous breaking surfable waves. Predictions of the wave height (H) at

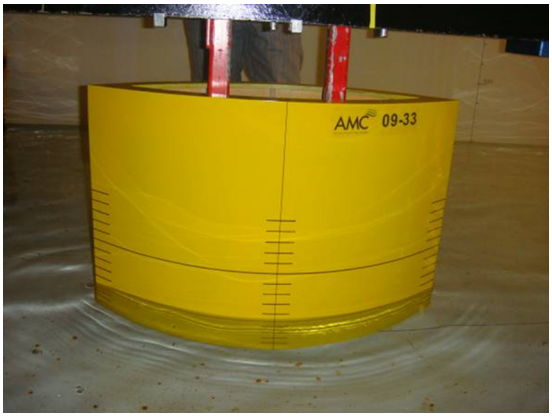

Fig. 3 Model 09–33 parabolic pressure source of 700 mm length, 300 mm beam, and 500 mm height

Fig. 4 Model 09–34 parabolic pressure source of 700 mm length, 600 mm beam, and 500 mm height

different Fr_h were first developed using two different methods: the Michlet panel method [9], and an empirical method developed by Verheij and Bogaerts [10]. Scale model tests were conducted in the 100 m long towing tank at AMC to validate the predictions.

Pressure Sources

Model 09-33 was a parabolic pressure source of 700 mm waterline length (*LWL*), 300 mm beam (*B*), and 500 mm height (see Fig. 3). The parabolic models were 500 mm deep to allow for up to 300 mm draft (*T*) and 200 mm freeboard to prevent overtopping.

The advantage of the wavedozer was believed to be that it may have been more efficient in generating waves than the parabolic pressure sources, as it primarily pushed vertically down on the free surface. The construction of the wavedozer was also relatively simple, being a wedge.

The pressure sources were configured as detailed below:

(a) The models were fixed in heave and trim.
(b) The pressure sources were initially tested with 100 mm draft. Drafts of 150 mm, 200 mm, 250 mm, and 300 mm were tested to investigate the effect on the wave height of the pressure source draft and displacement.

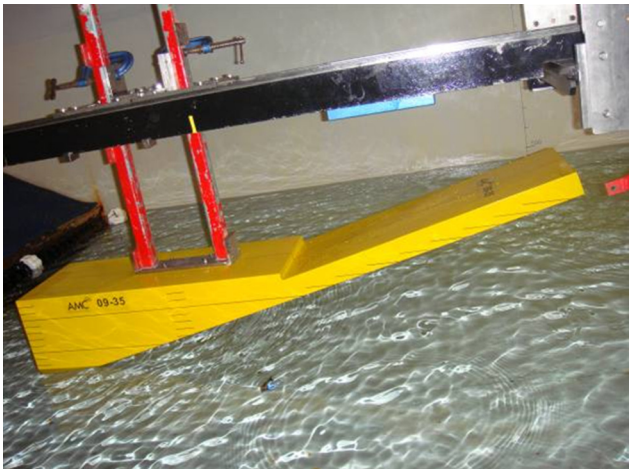

Fig. 5 Model 09–35 wavedozer pressure source of 1500 mm length, and 300 mm beam

Table 1 Test configurations—models tested for each set of conditions

	Draught (*T*) (mm)				
Water Depth (*h*) (mm)	100	150	200	250	300
200	09–33				
500	All				
600	All	All	All	09–35	09–35
700	09–33, 09–34		09–33		

(c) As symmetrical models were used, the wave measurements were taken on only one side (port).
(d) The test configurations used are detailed in Table 1.

Wave Probes

The wave probe (*WP*) setup, Fig. 6, was:

(a) The data from *WP2* was used to determine the surfable wave amplitudes. *H* of the first wave was measured from the trough to the crest.
(b) The array *WP2*, *WP4*, and *WP5* was used to determine the longitudinal stability of the waves.
(c) The array *WP1*, *WP2*, and *WP3* was used to determine the lateral changes of the waves.

The wave probes were in a fixed location 80 m (*WP1*, *WP2*, and *WP3*) from the start of tow tank. This distance was sufficient to allow the waves to reach a steady state before the pressure source passed the wave probes.

Errors

The calibration error for the wave probes was assumed to be ± 0.5 mm.

The repeatability error was calculated for the significant waves by repeating a number of test runs three times each. The worst case of ± 12.1 mm generated in a water depth of 500 mm was used. Note that the large error in water height is believed to be due to wave breaking occurring across the width of the tow tank.

By adding the calibration and the repeatability errors, a standard error for wave height of 12.6 mm was used. Note this error was a very conservative estimate; the true error is likely to be much lower. However, the high error estimate has been retained to ensure conclusions are significant.

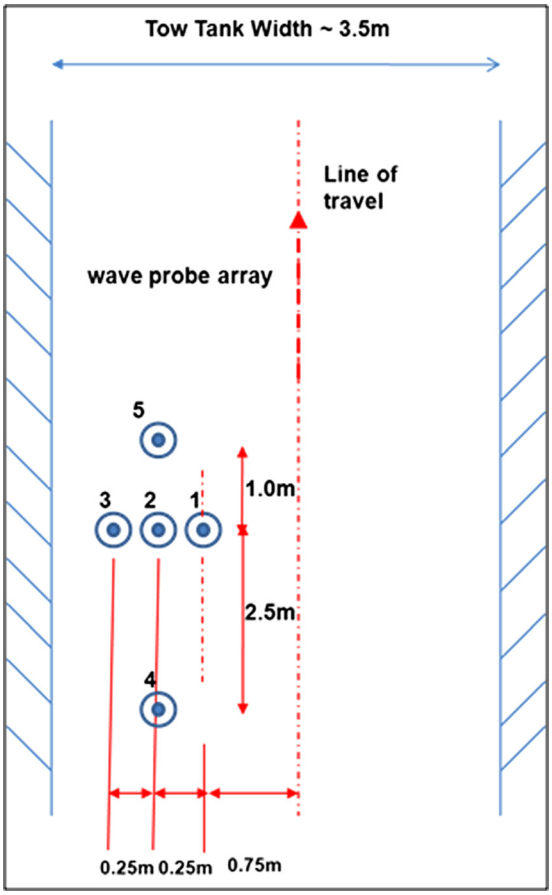

Fig. 6 The wave probe setup

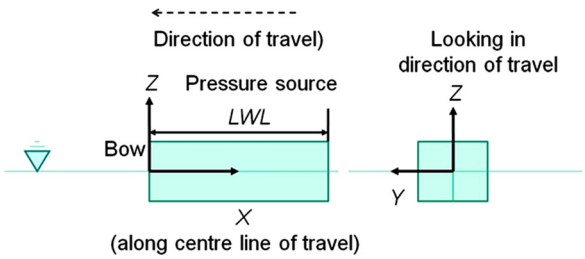

Fig. 7 Coordinates system

Although the waves were reflected off the tow tank walls after the runs were completed, by comparing the wave traces for *WP2*, *WP4*, and *WP5*, it was believed that the reflected waves were not affecting the wave probe results at *WP2*.

Coordinates System

The coordinates system used (Figs. 7 and 8), was:

(a) x was positive astern, y was positive to left (portside), and z was positive upwards.
(b) The undisturbed water surface was the plane $z=0$.
(c) The "bow" was defined as the forward extremity of the pressure source at the free surface for the static undisturbed water surface.
(d) *LWL* was defined as the distance between the forward and rear extremities of the pressure source at the free surface for the static undisturbed water surface.
(e) θ is the wave propagation angle, where $\theta=0$ corresponds to waves perpendicular to the pressure source's track (negative x-axis), with positive angles θ correspond to waves being propagated to the left (portside) of the body.

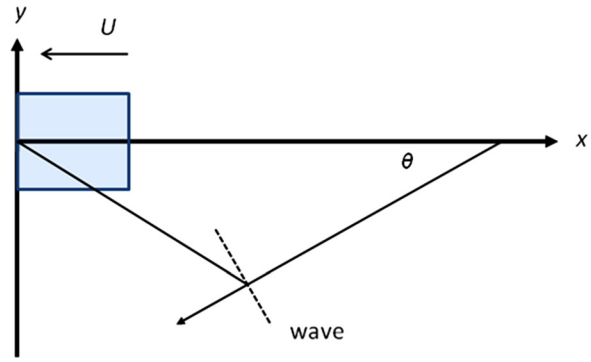

Fig. 8 Wave field coordinates

Michlet Potential Flow Model

An initial estimate of the required pressure source speed was determined by the authors as 5 m/s from a meta-analysis of existing surfing wave studies [11].

The next issue to be addressed was the suitability of a potential flow model to predict the waves generated by the pressure sources. The investigation used Michlet, a potential flow tool used for ship wave analysis [9]. Michlet had the advantage of being able to rapidly model a large number of test conditions. A rapid modeling method was required to conduct an initial analysis of the waves generated by the pressure sources given the freedom to control many of the design parameters, including pressure source configuration (shape, length, beam, draft, and displacement), water depth, and pressure source speed.

Michlet is based on Michell's thin-ship theory [12]. For a thin body with offsets $y=Y(x,z)$, where the local beam changes are small, Michell's theory indicates the amplitude function $A(\theta)$ [9], Eq. (1):

$$A(\theta) = -\frac{2i}{\pi}k_0^2\sec^4\theta\int\int Y(x,z)\exp(k_0 z\sec^2\theta + ik_0 x\sec\theta)dxdz \quad (1)$$

where the integral with respect to x is along the length of the body, and that with respect to z over the actual vertical position of the body. k_0 is the wave number of pure transverse waves at $\theta=0$ and equals g/U^2. The body and flow are assumed to have lateral symmetry, and then A(θ) is an even function and need only be computed for $\theta=>0$.

It is also equivalent to represent the body by a continuous distribution along the center-plane of dipoles (aligned in the x-direction) of moment proportional to the local width of the body [13], where σ is the moment (Nm) and U is the pressure source speed (m/s) (see Eq. (2)):

$$\sigma = 2UY(x,z) \quad (2)$$

As detailed in Ref. [14], the waves are created by a pressure source where there is a longitudinal change in the pressure source beam; the component of a pressure source where the waterline is parallel (flat sided) does not contribute to wave making. Therefore, this project aimed to test whether a pressure source design that has a continually changing beam would efficiently generate waves. Examples of this design were the hyperbolic tangent waterline pressure sources, with an *LWL* to *B* ratio of 1.3 and 1.75, used in initial investigation by Schipper [15] and Vries [16]. The design required the investigation to test and ultimately violate Michlet's *thin ship* assumption. Specifically, the error rate of wave heights predicted by Michlet to experimental results when using *nonthin* pressure sources was required.

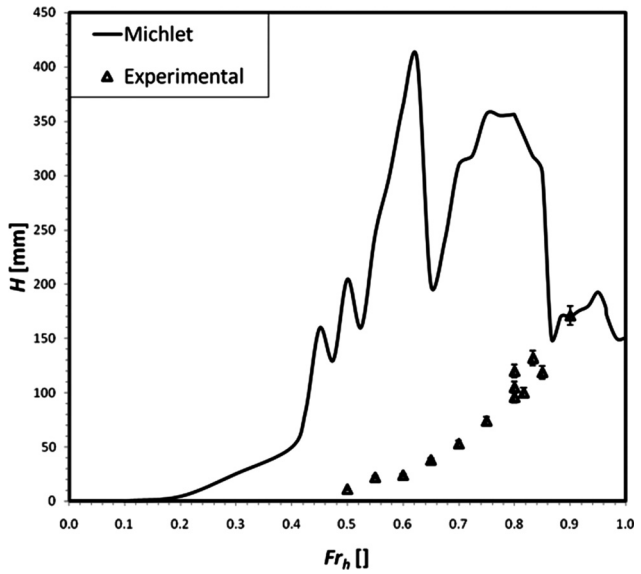

Fig. 9 *H* predicted using Michlet compared to the experimental results versus Fr_h at *WP1* for model 09–34 with 100 mm draft in 500 mm water depth

To provide additional experimental data to validate the ability to accurately predict the wave heights using Michlet, linear tow tank testing was conducted with the three models using combinations of Fr_h, water depth (h), and draft [17].

The wave amplitudes and heights predicted utilizing Michlet were generally found to be overestimated, by up to 400%, compared to the experimental results. An example of the overestimation is shown in Fig. 9 for model 09-34 in 500 mm water depth with 100 mm draft.

The overestimation of wave heights predicted using Michlet is believed to be due to Michlet being a panel method based on Michell's thin ship theory. Michlet uses three simplifications [9]:

(a) The velocities are linearized on the pressure source and free surface.
(b) The pressure source is modeled by a (known) continuous distribution of singularities along the center-plane of the thin body, requiring that the body does not have sudden changes in beam.
(c) Michlet does not include viscous drag, water kinematic viscosity, or eddy kinematic viscosity.
(d) Michlet does not handle breaking waves. However, the aim of the testing was to generate nonbreaking waves in the constant depth water. Wave breaking will be triggered by the addition of a beach in future testing.

Couser [18] suggested that the first two assumptions (linearized velocities and pressure source modeling) leads to the restrictions that the pressure source LWL / B be at least five and small longitudinal changes in beam are normally required for accurate wave height utilizing a *thin-ship* method such as Michlet.

This testing provided data to determine whether it was possible to predict waves generated by pressure sources with LWL / B less that five using Michlet. The LWL / B ratios for the tested pressure sources were:

(a) 2.34 for model 09-33.
(b) 1.17 for model 09-34.
(c) 1.34 for model 09-35 with 100 mm draft, and up to 4.01 with 300 mm draft, as LWL of the wavedozer is proportional to the draft.

It is believed that *nonthin* pressures sources, with LWL/B ratios less than five, may have contributed to the wave heights being overestimated due to Michlet utilizing a linear free surface. To overcome the linear free surface limitations, a nonlinear free surface model will be utilized for future analysis.

Empirical Prediction

H for values of $Fr_h < 1$ were calculated for each test series (combination of model, water depth and draft) using an empirical method by Verheij and Bogaerts [10] as shown in Eq. (3):

$$H = h \cdot \alpha_1 \left(\frac{y}{h}\right)^{-1/3} Fr_h^{\alpha_2} \tag{3}$$

where H (m) was predicted for h (m) at a lateral distance from the pressure source centerline (y) (m).

The wave generating ability of the pressure source shape is considered through a shape coefficient α_1 and a dimensionless wave height coefficient α_2. Verheij and Bogaerts [10] suggest $\alpha_1 = 1.2$ and $\alpha_2 = 4.2$ for blunt pressure sources. Verheij and Bogaerts [10] further defined in Eq. (4):

$$\alpha_1 = \alpha_2 \cdot T/Le \tag{4}$$

where T is the draft (m) and Le is the entry length (the distance from the bow to the parallel midship section (m). From Eq. (4), α_1 and α_2 were initially assumed to be 1.2 and 4.2, respectively, for all models.

Verheij and Bogaerts [10] stated that the assumptions for Eq. (3) are:

(a) Sub-critical speeds of $Fr_h < 0.7$.
(b) The waves should not break, with the wave breaking limit being $H / h > 0.6$.
(c) The pressure sources are limited to boat like shapes (tugs, barges, and motor boats).

In the testing reported in this paper, values of Fr_h up to 1.2 were tested, violating the water depth and speed limitations of $Fr_h < 0.7$. However, the equations for waves generated by the models for each test series (model, water depth, and draft) appeared to be able to be developed Fr_h up to 1. Although some scatter is present, a reasonable curve can be drawn, suggesting the wave height may be determined as a function of Fr_h.

While H / h remained less than the wave breaking limit of 0.6, the waves for models 09-33 and 09–34 did break for speeds where $Fr_h > 0.7$, while model 09–35 experienced minimal wave breaking for speeds where $Fr_h < 1$.

The experimental results (Fig. 10) for each pressure source with 100 mm draft in 500 mm water depth were plotted and an equation for the line of best fit derived to determine the wave generating coefficients α_1 and α_2(Table 2). The wave heights predicted by Eq. (3) utilizing the coefficients α_1 of 1.2 and α_2 of 4.2 are shown for comparison and to demonstrate that the form of Eq. (1) is applicable.

It is believed that once the wave generating coefficients for a pressure source is derived from the experimental results, the wave heights can be predicted for different values of Fr_h. However, it is believed that the physical reason that the coefficients are different for the models is that α_1 is determined by the bluntness of the pressure source, with 0 (no beam) $< \alpha_1 <$ 1.2 (blunt). Therefore, by utilizing $\alpha_1 = 1.2$, the bluntness of the models was overestimated. In reality, a different empirical equation, and the wave generating coefficients α_1 and α_2, are required to be developed from the experimental results for each test condition.

From Fig. 10, model 09–34 appeared to generate the largest waves for a given value of Fr_h. However, the waves generated by models 1 and 2 were broken across the entire tank width for speeds above $Fr_h > 0.75$, whereas the waves generated by model 09–35 exhibited minimal or no wave breaking for speeds up to $Fr_h < 0.95$.

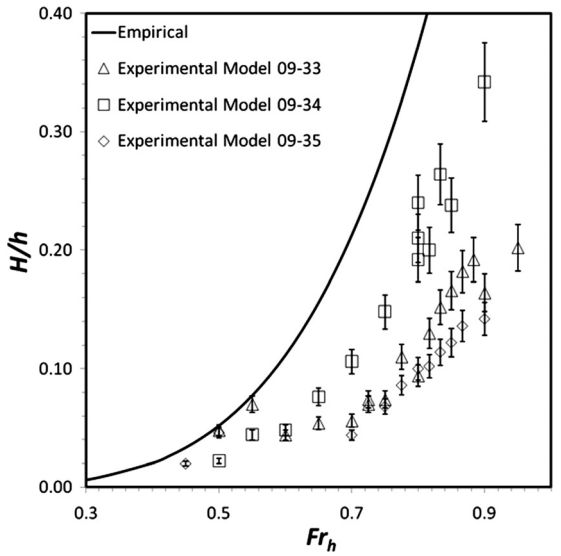

Fig. 10 The predicted values compared to the experimental results for *H* divided by *h* versus Fr_h for models 09–33, 09–34, and 09–35 in 500 mm water depth and 100 mm draft

Table 2 Wave generating coefficients for models 09–33, 09–34, and 09–35 with 100 mm draught in 500 mm water depth

Model	α_1	α_2
09–33	0.26	2.57
09–34	0.7	4.56
09–35	0.22	2.83

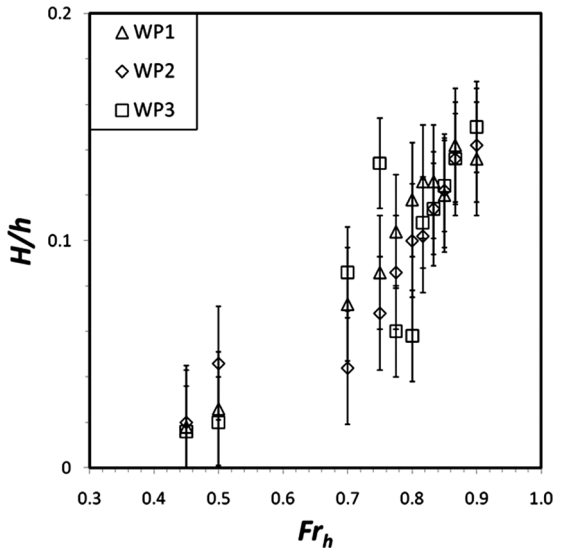

Fig. 11 Experimental results for *H* divided by *h* versus Fr_h for model 09–35 in 500 mm water depth with 100 mm draft at *WP1* ($y = 0.75$ m), *WP2* ($y = 1$ m) and *WP3* ($y = 1.25$ m)

Lateral Distance

To test whether the empirical method was valid for different lateral distances from the pressure source, the wave generating coefficients for model 09–35 with 100 mm draft in 500 mm of water were determined for *WP1* ($y = 0.75$ m), *WP2* ($y = 1$ m) and *WP3* ($y = 1.25$ m) (see Fig. 11 and Table 3).

Table 3 Wave generating coefficients of Model 09–35 at different lateral distances in 500 mm water depth with 100 mm draught

Lateral distance	α_1	α_2
WP1 ($y = 0.75$ m)	0.27	3.67
WP2 ($y = 1$ m)	0.22	2.83
WP3 ($y = 1.25$ m)	0.3	3.84

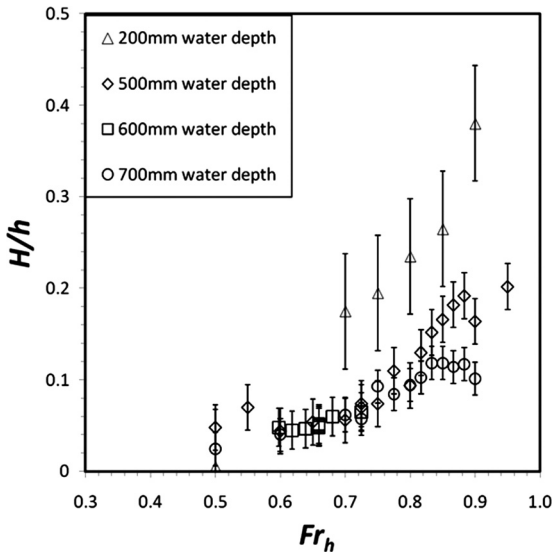

Fig. 12 Experimental results for *H* divided by *h* versus Fr_h for model 09–33 at *WP2* with 100 mm draft in 200 mm, 500 mm, 600 mm, and 700 mm water depth

The large variation in the results for *WP3* may be due to the interaction of the transverse and divergent waves at certain values of Fr_h and reflections from the tank wall. Thus it is believed that the wave generating coefficients of the models may not be valid for different lateral distances from the pressure source center line of travel, given the underlying error within the results.

Water Depth

To test whether the wave generating coefficients of the models are valid for different values of *h*, the coefficients for model 09–33 with 100 mm draft were compared for 200 mm, 500 mm, 600 mm, and 700 mm water depth at *WP2* ($y = 1$ m) (see Fig. 12 and Table 4).

It is believed that the wave generating coefficients for 200 mm water depth were not valid as the results for the wave generating coefficients are larger than the maximum values detailed by Verheij and Bogaerts [10]. Waves with a larger H / h ratio were generated for the shallower water depth (500 mm) for given values of Fr_h; however, as the waves were breaking for $Fr_h > 0.75$, the results were found to inconclusive.

Table 4 Wave generating coefficients of model 09–33 with 100 mm draught in different water depths

Water depth (mm)	α_1	α_2
200	2.03	7.35
500	0.26	2.57
600	0.13	1.85
700	0.19	2.81

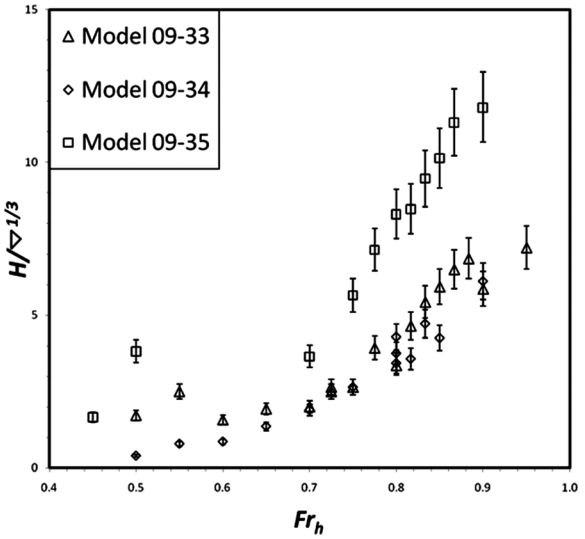

Fig. 13 Experimental results for *H* at *WP1* divided by the cubic root of displacement volume ($\nabla^{1/3}$) versus Fr_h for the models 09–33, 09–34, and 09–35 with 100 mm draft in 500 mm water depth

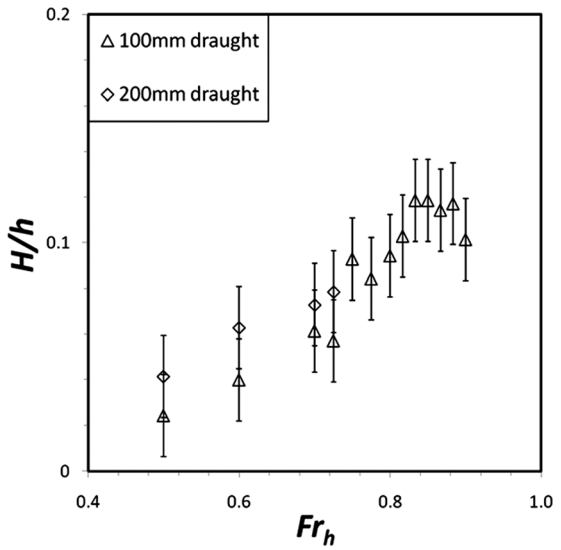

Fig. 14 Experimental results for *H* divided by *h* versus Fr_h at *WP2* for model 09–33 in 700 mm water depth with 100 mm and 200 mm draft

Table 5 Wave generating coefficients of model 09–33 with different draughts in 700 mm water depth

Draught (mm)	α_1	α_2
100	0.19	2.81
200	0.15	1.65

Lastly, it is believed that blockage, being the pressure source cross sectional area to the channel cross sectional area, may also be affecting the results. Increased blockage may increase the wave heights generated, but also trigger wave breaking.

Draught / Displacement

The three models with a draft of 100 mm had displacement volumes (∇) of 0.014 m^3, 0.028 m^3 and 0.006 m^3 for models 09–33, 09–34, and 09–35, respectively. Subsequently, the wave heights divided by the cubic root of displacement volume ($H/\nabla^{1/3}$) were calculated as an indication of the energy efficiency (a smaller volume pressure source to generate a given height wave) (see Fig. 13).

Model 09–35 generated the largest wave heights for a given value of ∇, with models 09–33 and 09–34 generating approximately the same height waves for a given value of ∇. This result may indicate that model 09–35 is a more efficient wave generator, requiring a smaller volume pressure source to generate a given design height wave. However, actual power requirements will be need to be determined in the future.

To test whether the wave generating coefficients of the models are valid for different drafts, the wave heights were compared for model 09–33 in 700 mm water depth with 100 mm and 200 mm draft (Fig. 14 and Table 5).

From Table 5, it is recommended that both the coefficients α_1 and α_2 need to be determined for each value of draft. Furthermore, it is believed that wave heights generated increased with the pressure source draft for a given value of Fr_h. Moreover, the relationship between wave height and pressure source draft could not be directly determined for model 09–35 as *LWL* increased proportional to the draft.

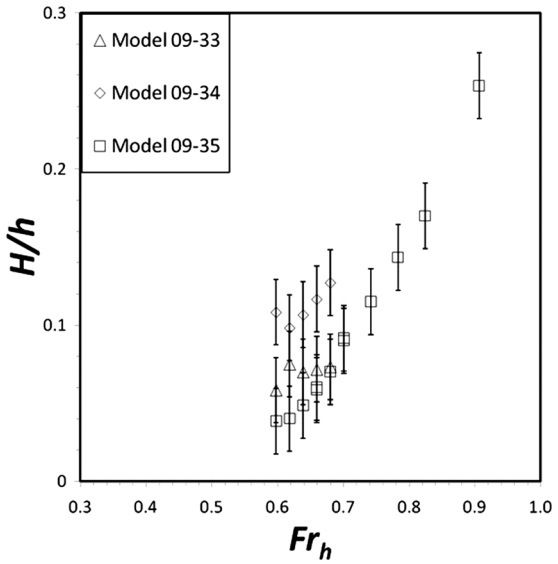

Fig. 15 Experimental results for *H* divided by *h* versus Fr_h for models 09–33, 09–34, and 09–35 with 200 mm draft in 600 mm water depth

Wave Comparison

To determine which model generated the highest waves, the waves generated by the models with the same draft and water depth were compared.

As previously shown in Fig. 10, the wave heights for all models with 100 mm draft in 500 mm water depth increase with increasing values of Fr_h up to 1.0, with model 09–34 generating the largest waves. However, the waves generated by models 09–33 and 09–34 broke across the entire tank width for $Fr_h > 0.75$, whereas the waves generated by model 09–35 exhibited minimal or no wave breaking for $Fr_h < 0.95$.

To test the relationship at higher blockages (3% for models 09–33 and 09–35, and 6% for models 09–34, compared with 1.5% for models 09–33 and 09–35 and 3% for models 09–34 in Fig. 10), the waves generated by the three models with 200 mm draft in 600 mm water depth were determined (Fig. 15).

From both Figs. 10 and 15, model 09–34 appears to generate the largest waves for a given Fr_h, with models 09–34 and 09–35 (with the same beam) generating waves of approximately the

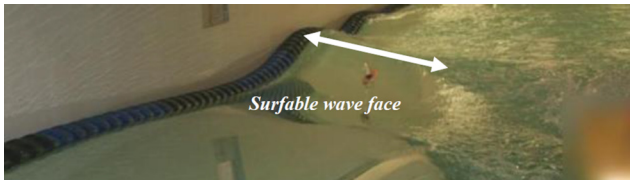

Fig. 16 Quality waves generated for model 09–35 in water depth of 600 mm with 200 mm draft at $Fr_h = 0.907$

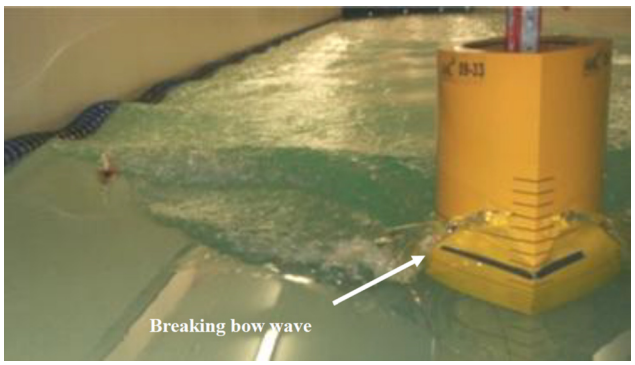

Fig. 17 Breaking bow wave generated for model 09–33 in water depth of 600 mm with 100 m draft at $Fr_h = 0.8$ with wash guard fitted

same height. However, as stated earlier, the waves generated models 09–33 and 09–34 broke across the entire width of the channel for $Fr_h > 0.75$.

Nevertheless, as model 09–34 appears to generate larger waves than model 09–33 at a given speed, water depth, and draft, this suggests that larger waves can be generated by utilizing a pressure source with a wider beam and therefore greater blockage.

However, the waves generated by the model 09–35 increased in height as Fr_h approached 1 without significant wave breaking. As such, model 09–35 may be able to generate the largest nonbreaking waves by utilizing a speed in the range of $0.9 < Fr_h < 1.0$, with even larger waves possibly generated by increasing the beam, and therefore blockage. The largest smooth waves generated were model 09–35 with 300 mm draft in 600 mm water at $Fr_h = 0.9$, with $H = 183$ mm (4% blockage).

Wave Quality

As stated earlier, the quality of the waves generated is critical for their usability for surfing, and without the presence of a beach, the waves generated by the pressure source should remain unbroken. As an example of a good quality wave, Fig. 16 shows a large unbroken wave of height generated utilizing model 09–35 in water depth of 600 mm with 200 mm draft at $Fr_h = 0.907$, where the surfer may ride on the wave face between the wall and the bow wash.

Model 09–35 generated good quality waves with 100 mm and 200 mm draft and speed in the range $0.598 <= Fr_h <= 0.948$. Again, models 09–33 and 09–34 appear to be limited to speeds of $Fr_h < 0.75$ for the generation of quality waves, due to wave breaking across the entire width of the tow tank above Fr_h.

The maximum number of smooth sinusoidal waves generated was seven for model 09–33 in 700 mm water depth with 200 mm draft at $Fr_h = 0.5$, however, these waves were very small.

For all three models, the number of smooth sinusoidal waves generated decreased with increased Fr_h, with only to 1 or 2 waves generated for $Fr_h > 0.8$. It was noted that model 09–35 generally generated more smooth waves that models 09–33 and 09–34 at the same Fr_h.

Furthermore, a large breaking bow wave was formed by models 09–33 and 09–34 for $Fr_h > 0.6$ (Fig. 17). This bow wave is undesirable as it adversely interacts with the smooth ship waves, and effectively reduces the wave generating efficiency of the pressure source.

Concluding Remarks

From this work, the following conclusions were drawn:

(a) *Michlet*. To overcome linear free surface limitations, a nonlinear free surface model will be utilized for future analysis.
(b) *Empirical method*. Once the wave generating coefficients of a pressure source were derived from the experimental results, the wave heights may be predicted for different values of Fr_h. However, the predicted results may not be valid if different water depths or lateral distances from the pressure source centerline of travel are used.
(c) *Beam*. For a given Fr_h, water depth, and draft, a larger beam (between model 09–33 and 09–34) generated an increase in wave height.
(d) *Displacement*. The wavedozer generated the largest wave heights for a given displacement.
(e) *Wave heights*. For $Fr_h < 1.0$, model 09–34 generated the largest waves. However, since both model 09–33 and 09–34 generated waves that broke across the entire tank width for $Fr_h > 0.75$, the preferred pressure source to generate the maximum wave height without significant wave breaking was model 09–35 within the speed range of $0.9 < Fr_h < 1$. Furthermore, it may be possible for model 09–35 to generate with larger waves possibly by increasing the beam, and thus blockage.
(f) *Surf quality*. The largest smooth waves were generated by model 09–35 at $Fr_h <= 0.948$. The next stage of this work was to design and build a circular test facility to enable the difference in wave generation characteristics for pressure sources moving in a circular path compared to a straight path to be investigated experimentally.

Nomenclature

α_1 = shape coefficient
α_2 = dimensionless wave height coefficient
θ = wave propagation angle
σ = moment
∇ = displacement volume
$A(\theta)$ = amplitude function
B = pressure source beam
Fr_h = depth Froude number
g = gravitational acceleration
H = wave height
h = water depth
k_0 = wave number of pure transverse waves at $\theta = 0$. $k_0 = g/U^2$
LWL = pressure source waterline length
Le = pressure source entry length
T = draft
U = pressure source speed
$x; y; z$ = coordinates of a point in the wave field
Y = pressure source body offset
WP = wave probe

Acknowledgment

The authors would like to acknowledge the support of our industry partner Webber Wave Pools. We would also like to acknowledge the support of the Australian Maritime College technical team, and our fourth year students Nathan Doyle and James Erbacher.

The authors would also like to acknowledge the support of Leo Lazauskas, who developed the Michlet program and provided valuable advice on the utilization of Michlet for our project.

Finally, the authors would like to acknowledge the support of the Australian Research Council through their award of our Linkage Project Grant No. LP0990307.

References

[1] Wright, D., 2003, "Economics of Surf Reefs," Proceedings of the 3rd International Surfing Reef Symposium, Raglan, New Zealand, pp. 351–359.
[2] Wicker, C., 2007, "Everything You Need to Know About Wave Pools," retrieved Dec. 31, 2009, http://www.surfshot.com/In+A+Minute/Everything+you+need+to+know+about+Wave+Pools+-141833.html
[3] Aquatic Development Group, 2005, "Real Surfing: Custom Designed Wave Pools for the Ultimate Surfing Experience," retrieved Dec. 30, 2009, www.aquaticgroup.com
[4] Waveloch, 2009, "Flowrider Single," Retrieved Dec. 29, 2009, http://www.waveloch.com/attraction/flowrider-single
[5] Waveloch, 2009, "Flying Reef and Moving Reef," Retrieved Dec. 29, 2009, http://www.waveloch.com/attraction/flying-reef-and-moving-reef
[6] Webber, G. M., 2004, Australian Patent No. 20049070401, Intellectual Property Australia, Canberra.
[7] Webber, G. M., 2006, International Patent No. WO/2006/060866, World International Patent Organization, Geneva, Switzerland.
[8] Schmied, S., and Meier, M., 2007, "Surfin 'in Circles," Eng. World, Dec 2007/Jan 2008, pp. 30–33.
[9] Tuck, E. O., Lazauskas, L., and Scullen, D. C., 1999, "Sea Wave Pattern Evaluation, Part 1 Report: Primary Code and Test Results (Surface Vessels)," Report to the Applied Mathematics Department, University of Adelaide, Australia, pp. 1–10.
[10] Verheij, H. P., and Bogaerts, M. P., 1989, "Ship Waves and the Stability of Armour Layers Protecting Slopes," Publication No. 428, Delft Hydraulics, Delft, The Netherlands.
[11] Schmied, S. A., Binns, J., Renilson, M. R., Thomas, G., Macfarlane, G., and Huijsmans, R., 2010, "A Novel Method for Generating Continuously Surfable Waves," Mar. Technol. Soc. J., **44**(2), pp. 7–12.
[12] Michell, J. H., 1898, *The Wave Resistance Of A Ship*, Philos. Mag., **45**, pp. 106–123.
[13] Tuck, E. O., Lazauskas, L., and Scullen, D. C., 1999, "Sea Wave Pattern Evaluation, Part 2 Report: Investigation of Accuracy," Report to the Applied Mathematics Department, The University of Adelaide, Australia, pp. 1–28.
[14] Lazauskas, L., 2012, Michlet version 9.20, 2011, "Michlet Software Manual, mlt806_verification.xls (NPL Rt worksheet)," http://www.cyberiad.net/michlet.htm
[15] Schipper, M. A., 2007, "On the Generation Of Surfable Ship Waves in a Circular Pool: Part I Physical Background & Wave Pool Design," M.S. thesis, Faculty of Civil Engineering and Geosciences, Delft University of Technology, Delft, The Netherlands.
[16] Vries, S. D., 2007, "On the Generation Of Surfable Ship Waves in a Circular Pool, Part II," M.S. thesis, Faculty of Civil Engineering and Geosciences, Delft University of Technology, Delft, The Netherlands.
[17] Schmied, S. A., 2010, "Test Report: Tow Tank Testing From 21 December 2009 – 1 January 2010," University of Tasmania, Sandy Bay, Australia.
[18] Couser, P., 1996, "An Investigation into the Performance of High-Speed Catamarans in Calm Water and Waves," Ph.D. thesis, Department of Ship Science, University of Southampton, Southampton, UK.